AN X-RAY SCATTERING INVESTIGATION OF WILD CUCUMBER MOSAIC VIRUS AND A RELATED PROTEIN

J. W. ANDEREGG, P. H. GEIL, W. W. BEEMAN, *and* PAUL KAESBERG

From the Physics Department and the Biochemistry Department, University of Wisconsin, Madison. Dr. Geil's present address is Polychemicals Department, du Pont Experimental Station, Wilmington.

ABSTRACT X-ray scattering data are presented on solutions of wild cucumber mosaic virus and the associated "top component" particles which have little or no RNA. The radii of gyration are 112 Å and 135 Å for bottom and top component, respectively. The radial density distribution within each particle is calculated by Fourier inversion of the scattered amplitudes. The virus particle or bottom component has approximately uniform density with an outer radius of about 140 Å. The transform of the top component shows an almost hollow center extending out to 105 Å with a surrounding shell of high density about 35 Å thick. Thus the RNA would appear to occupy the region inside 105 Å and does not overlap appreciably the region occupied by protein. The virus has associated with it approximately 0.38 gm of water per gm of virus, resulting in an average electron density of 1.25 times that of water.

INTRODUCTION

Several viruses are known to cause their infected hosts to produce virus-like particles as well as additional virus. Comparison of the biophysical and biochemical properties of such particles with their corresponding virus particles has yielded more extensive structural information than would have been obtainable from studies of the viruses alone. The classical example is turnip yellow mosaic virus (TYMV) which induces the production of a protein antigenically similar to the virus but which is non-infectious and contains no nucleic acid (Markham and Smith, 1949). Since this particle sediments more slowly than the virus it was called the top component. Markham (1951) found that the top component had the same diameter and surface properties as the virus and concluded on this basis that the virus consisted of a protein shell with a nucleic acid core and that the top component consisted of only the protein shell. X-ray scattering data bore out this view

(Schmidt, Kaesberg, and Beeman, 1954). The scattering from the virus indicated a uniform sphere of diameter 280 Å and the scattering from the top component indicated a hollow shell 280 Å in outside diameter and 35 Å thick.

Infection with wild cucumber mosaic virus (WCMV) causes the production of two kinds of virus-like particles in addition to virus (Yamazaki and Kaesberg, 1961*a*). These are designated top component *a* and top component *b*. The virus (*i.e.* bottom component) has a molecular weight of 7.0×10^6 and an RNA content of molecular weight about 2.4×10^6. Top component *b* weighs 4.4×10^6 and contains 0.48×10^6 molecular weight of RNA. Top component *a* has a molecular weight of 4.0×10^6 and is devoid of RNA. All three particles have a similar amino acid composition and the RNA in top component *b* and bottom component have a similar base composition. Bottom component can be separated from the top components by means of density gradient sedimentation in sucrose solutions. Satisfactory separations of top component *a* and top component *b* have not been achieved because they have nearly equal sedimentation rates (53S and 62S) and similar chemical properties. Their mixture is designated top component.

Previous communications from this laboratory have reported x-ray scattering investigations of solutions of four spherical viruses: southern bean mosaic virus, tobacco necrosis virus, and tomato bushy stunt virus (Leonard, Anderegg, Shulman, Kaesberg, and Beeman, 1953), and top and bottom components of turnip yellow mosaic virus (Schmidt *et al.*, 1954).

This paper reports x-ray scattering data on top and bottom components of WCMV. An attempt is made to obtain detailed information about the structure of these particles by calculating the radial electron density distribution within the particles from the Fourier transform of the scattered amplitudes.

THEORY

The intensity $I(h)$ of scattered x-rays from a nearly random collection of identical particles, as in a dilute solution, is proportional to the diffraction pattern of a single particle averaged over all orientations of the particle with respect to the incident beam. That is

$$I(h) = NI_e(h)\overline{F^2(h)} \tag{1}$$

where $h = 4\pi \sin \theta/\lambda$, 2θ is the scattering angle, λ is the x-ray wave length, N is the number of particles in the scattering volume, and $I_e(h)$ is the intensity scattered by a single electron. $F(h)$ is the structure factor of the particle and is the ratio of the amplitude scattered by the particle to the amplitude scattered by a single electron. The bar over $F^2(h)$ indicates the averaging over all orientations. By considering a continuous charge distribution throughout the particle one can write

$$\overline{F^2(h)} = \int_v \int_v \rho_m \rho_n \frac{\sin hr_{mn}}{hr_{mn}} dv_m \, dv_n \tag{2}$$

where ρ_m is the electron density in the volume element dv_m and r_{mn} is the separation of volume elements dv_m and dv_n.

For a particle with spherical symmetry the value of $F(h)$ is independent of the orientation of the particle and one can write

$$F(h) = \int_0^R \rho(r) \frac{\sin hr}{hr} 4\pi r^2 \, dr \tag{3}$$

R is the radius of the particle; $\rho(r)$ is the electron density at a distance r from the center of the particle and can be determined by a Fourier transform of $h \cdot F(h)$. The magnitude of $F(h)$ can be determined from the square root of the scattered intensities but the sign must be determined from some additional information.

For all particles at very small angles

$$\overline{F^2(h)} = n^2 e^{-(h^2 R_g^2/3)} \tag{4}$$

where n is the total number of electrons in the particle and R_g is the radius of gyration or the root mean square distance of all the electrons from the center of charge of the particle. As the concentration of particles increases the interference between x-rays scattered from neighboring particles increases. This has the effect of decreasing the apparent radius of gyration as determined from the slope of the curve of log $I(h)$ *versus* h^2. Hence, to obtain the true radius of gyration one must measure the apparent value at a number of concentrations and extrapolate to infinite dilution.

EXPERIMENTAL

The x-ray source was a rotating copper anode tube operating at 30 kilovolts and 80 milliamps. Two different collimating systems were used. In the first (Beeman, Kaesberg, Anderegg, and Webb, 1957, p. 364) the x-ray beam incident on the sample was collimated with a pair of tantalum slits and the scattered beam was analyzed with a second pair of slits which rotated about an axis through the sample. The slits were 1 cm high with widths in the range from 0.01 to 0.05 cm. Successive slits were separated by 50 cm. The sample was placed midway between the second and third slits. In the second apparatus (Beeman *et al.*, 1957, p. 369) the beam was collimated by two pinhole apertures, each 0.05 cm in diameter, separated by a distance of 30 cm. The sample and a guard aperture were placed 15 cm beyond the second collimating pinhole. The scattered beam was detected with a large window proportional counter with an annular aperture 2 cm in diameter and 0.1 cm wide located in front of the counter, permitting only the x-rays scattered into a cone of a given angle to pass. The scattering angle was changed by changing the distance from sample to annular aperture. The space between the sample and annular aperture was evacuated and their separation made adjustable using telescoping brass tubes. The sample holders were made of lucite spacers 1 mm thick with thin mica windows. Monochromatization of the x-rays was obtained by making use of the proportional counter and a single-channel pulse-height analyzer with a 6 volt channel centered on the Cu K_α pulses which were adjusted to a height of 14 volts. A nickel filter reduced the intensity of Cu K_β radiation to about 3 per cent of Cu K_α.

The data were corrected for the smearing effects due to the height and width of the slits or the width of pinholes and annular aperture. The general techniques for these corrections have been reviewed by Beeman *et al.* (1957) and details of the particular methods used for this work are given elsewhere by Geil (1956). The numerical calculations were carried out on an IBM 650 computer. Background runs were made with solvent only in the sample holder and this background was subtracted from all data.

The purification and separation of top and bottom components of WCMV are described elsewhere (Sinclair *et al.*, 1957, and Yamazaki and Kaesberg, 1961*a*). The top component used was a mixture containing approximately 3 parts of top component *a* to 1 part of top component *b*.

RESULTS

Bottom Component. To eliminate interparticle interference effects from the scattering data and to obtain the true radius of gyration of the virus, the small-angle portion of the scattering curve was run at a series of concentrations decreasing from 0.6 per cent. The results for the apparent radius of gyration as a function of concentration and the extrapolation to zero concentration are shown in Fig. 1.

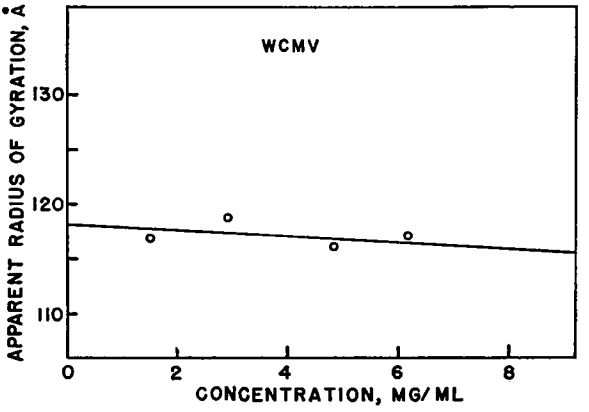

FIGURE 1 Apparent radius of gyration of wild cucumber mosaic virus as a function of virus concentration and the extrapolation to zero concentration.

The extrapolated value of the radius of gyration is 118 Å. Corrections (Beeman *et al.*, 1957, p. 354) due to the effect of the height of the collimating slits and to the deviations from a true Gaussian curve lower this result to 112 Å. A uniform sphere with this radius of gyration would have a diameter of 290 Å.

For studying the shape of the scattering curve at larger angles, where the scattered intensities were rapidly decreasing, it was necessary to use more concentrated solutions. The scattering from a 4 per cent solution was investigated out to an angle of 0.1 radian with slit collimation and a 3 per cent solution was investigated out to 0.08 radian with pinhole collimation. These were found to be in good agreement after correcting both curves for effects due to the non-zero size of the

collimating apertures. The small-angle portion of the curve was corrected for interparticle interference effects with the aid of the runs on dilute solutions. The resultant scattering curve is shown in Fig. 2. It should be noted that the intensities are on a log plot and that the intensity range covered by the data involves a factor of nearly 10^5. Besides the strong central maximum there are thirteen other maxima in the scattering curve. Experimental points are not shown because the data have been smoothed and slit-corrected, but the peaks shown are all reproducible. It is

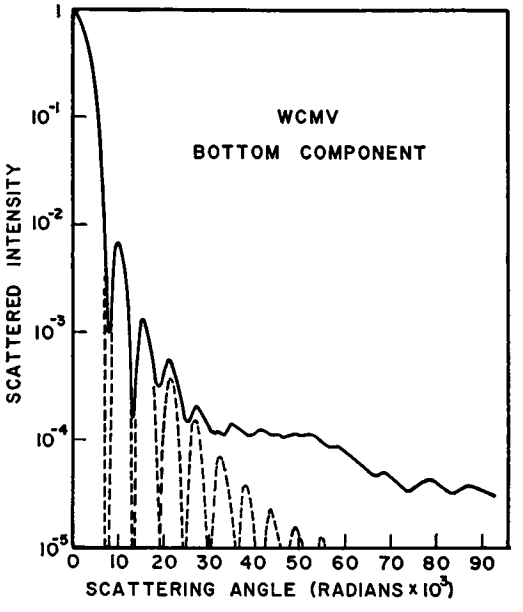

FIGURE 2 The intensity of x-rays scattered by a solution of wild cucumber mosaic virus as a function of scattering angle. The scattered intensities are on a log plot because of the large intensity range. The solid line representing the experimental data is a composite of data taken with several different slit widths and has been corrected for the effects due to the size of the slits. The dashed curve is the theoretical scattering curve for a uniform sphere of 140 Å radius.

seen that the central maximum and first two subsidiary maxima agree well with those in the scattering curve of a uniform sphere of radius 140 Å and after that agreement becomes progressively worse. This indicates that at low resolution the virus approximates such a sphere but that at higher resolution differences become noticeable. An outstanding feature of the experimental curve is the large plateau from 0.035 to 0.055 radian. The peaks at 0.078 and 0.087 radian correspond to Bragg spacings of 20 Å and 18 Å, respectively.

Top Component. Because less top component was available than bottom component, radius of gyration determinations were made on only two solutions each at 0.3 per cent concentration. The average radius of gyration determined

from these two solutions was 143 Å. Judging from the data on bottom component the correction to this result due to interparticle interference should be within the experimental error of approximately 3 per cent. Corrections due to the effect of slit heights and deviations from a Gaussian curve lower the result to 135 Å.

The scattering curve resulting from a composite of the slit and pinhole data after correction for collimation errors is shown in Fig. 3. Again there is a strong central maximum and, in this case, twelve additional maxima. The central maximum is

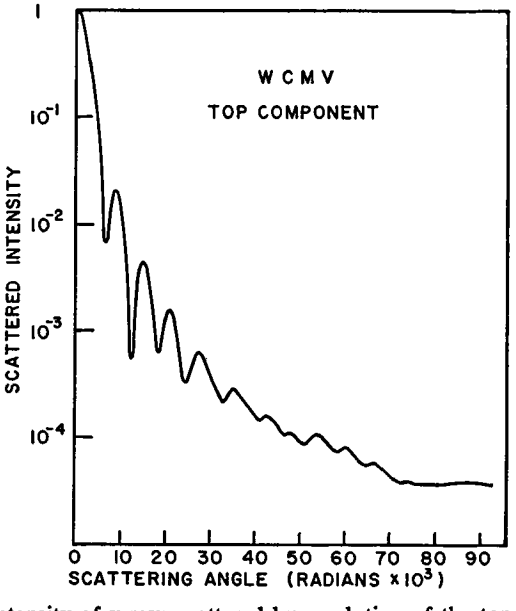

FIGURE 3 The intensity of x-rays scattered by a solution of the top component from plants infected with wild cucumber mosaic virus. The curve is a composite of data taken with different slit widths and has been corrected for slit effects.

narrower than that for bottom component; the ratio of the intensity of the central maximum to the intensity of the first five subsidiary maxima is much less for top component than it is for bottom. These deviations from the curve for bottom component and from the theoretical curve for a uniform sphere are in the direction to be expected for a hollow sphere. The central maximum and the first two subsidiary maxima are in reasonable agreement with a hollow sphere whose inner radius is 0.7 times the outer radius. The large plateau in the region from 0.035 to 0.06 radian and the peaks at 0.078 and 0.087 radian which were present in the scattering from bottom component are missing in the top component curve.

Fourier Transforms. Both top and bottom components of WCMV appear roughly spherical in electron micrographs (Sinclair *et al.*, 1957). Pictures of frozen-dried preparations provide evidence that the particles have a polyhedral shape but since the number of faces indicated is quite large (at least twelve) the

spherical approximation is still quite good. In addition the x-ray scattering curves are in qualitative agreement with those to be expected for spherical particles. For these reasons it seemed worth while to proceed under the assumption that both particles when looked at with poor resolution would exhibit spherical symmetry. In such a case the Fourier transforms of the scattering amplitudes should give a picture of the radial density distribution within the particles (Equation 3). For this calculation the signs of the scattering amplitudes must be determined by some in-

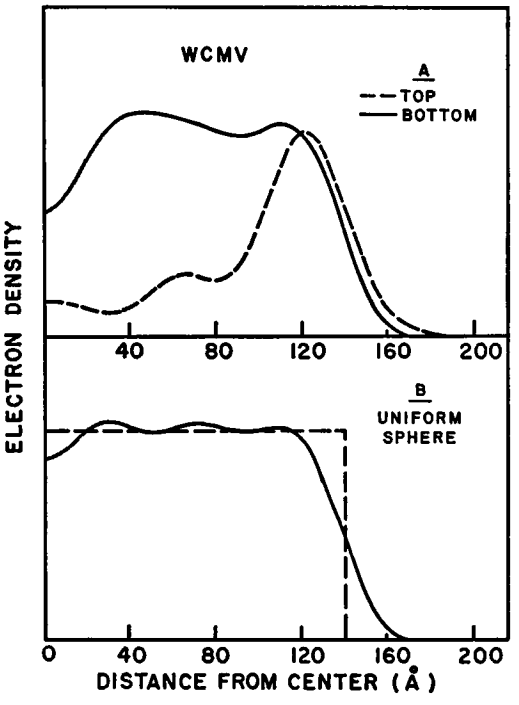

FIGURE 4A The radial distribution of electron density inside wild cucumber mosaic virus (solid curve) and the associated top component particle (dashed curve) as calculated from the Fourier transform of the scattered amplitudes.

FIGURE 4B The Fourier transform (solid curve) of the theoretically calculated scattering amplitudes from a uniform sphere of 140 Å radius. For comparison with the transform in (A) the amplitude curve was cut off at the same angle and multiplied by the same artificial temperature factor. The dashed line represents the uniform density distribution which would have resulted if the entire amplitude curve had been used in the inversion.

dependent means. The sign of the amplitudes in the central maximum may be taken to be positive. It is known that for uniform spheres and hollow spheres the succeeding maxima alternate in sign. For this reason it was assumed that the signs alternate for the first five maxima of the WCMV curves. The data beyond the fifth maximum could not be used in the Fourier inversions, since increasing irregularity

of the curves made sign determination ambiguous. The curves, even after collimation correction and background subtraction, did not go to zero at the minima. Possible reasons for this could be impurities in the preparation or, more likely, deviations from spherical symmetry of the scattering particles. Since both of these effects would fill in the minima without significantly changing the rest of the curve, the data near the minima were ignored and smooth curves drawn through the remaining data. Before making the Fourier inversion the scattering curves were multiplied by an artificial temperature factor to minimize the spurious diffraction effects due to the cut-off of the data beyond the fifth maximum. The temperature factor used was a Gaussian with the constant chosen so as to multiply the data by a factor of 0.1 at the cut-off point.

The radial density distributions obtained by Fourier inversion of the scattering amplitudes are shown in Fig. 4A. The resolution in these distributions is of the order of 40 Å. For comparison purposes the theoretical scattering curve for a uniform sphere of radius 140 Å was cut off after five maxima, multiplied by the same temperature factor, and the Fourier transform calculated. The result is shown in Fig. 4B. The dashed line represents the uniform density distribution which would have resulted if the entire amplitude curve had been used in the inversion. This gives an indication of the magnitude of the spurious diffraction effects and of the smearing due to poor resolution which are present in the density distributions. Clearly the small peaks in the curve for top component are not significant but the general features of both curves are meaningful.

The transform of the bottom component data shows a reasonably uniform density distribution and an outer radius of about 140 Å. The density curve for top component shows an almost hollow center extending out to 105 Å with a surrounding shell about 35 Å thick, giving an outer radius nearly the same as that of the bottom component. Thus the nucleic acid in WCMV appears to fill rather uniformly the region inside a radius of 105 Å but perhaps leaving a small hole of about 40 Å diameter in the center of the particle. The nucleic acid core is surrounded by a protein shell about 35 Å thick.

Hydration. If it is assumed that the partial specific volumes of the RNA and the protein of the intact virus are the same as for the free components, then the volume of water displaced by each component can be calculated by multiplying the molecular weight of the component times its partial specific volume. Assuming values (Yamazaki and Kaesberg, 1961*a*) of 2.4×10^6 and 0.54 for the molecular weight and partial specific volume of the RNA of WCMV and 4.0×10^6 and 0.74 for the corresponding properties of the protein, then the volumes of water displaced by the RNA and the protein of WCMV are 2.2×10^6 Å^3 and 4.9×10^6 Å^3, respectively. These compare with volumes of 4.9×10^6 Å^3 and 6.7×10^6 Å^3 for the core and the shell of the virus as calculated from the dimensions given in the last section. The difference in each case can be assumed to be occupied with water

of normal density. Thus one calculates that there is 0.26 gm of water per gm of protein in the shell and 0.68 gm of water per gm of RNA in the core, giving a total hydration of 0.38 gm of water per gm of virus. These hydrations indicate an average electron density in the core of 1.32 times that of water, an average electron density in the shell of 1.21 times that of water, and an average electron density for the whole virus of 1.26 times that of water. Since the transform in Fig. 4 represents the electron density above that of water, it is clear that the transform indicates a smaller density difference between core and shell than that just calculated. This disagreement cannot be taken too seriously, however, since the result is very sensitive to the value used for the radius of the core. Increasing the core radius from 105 A to 110 A would indicate equal electron density for core and shell.

The above result for the average electron density of the whole virus was checked by an independent determination. The intensity of the x-ray scattering in the forward direction from a molecule in solution is proportional to the square of the difference between the average electron density of the molecule and the electron density of the solvent. The electron density of the solvent can in effect be varied by

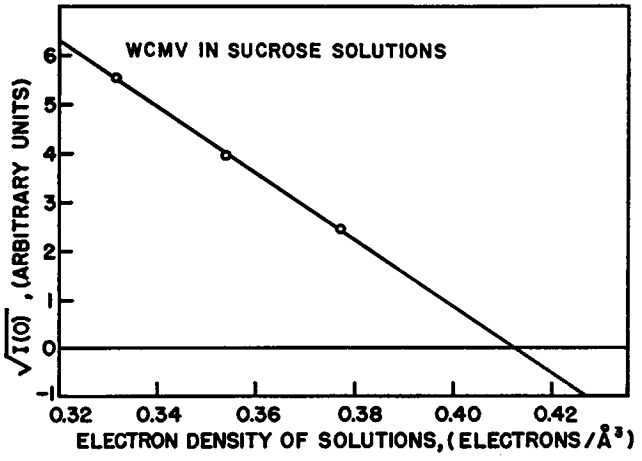

FIGURE 5 The square root of the intensity of x-rays scattered in the forward direction by WCMV in sucrose solutions. The results are plotted as a function of the electron density of the solution which is determined by the sucrose concentration. The extrapolation to zero intensity is shown.

adding a small molecular weight compound such as sucrose to the solution. The scattered intensity in the forward direction, $I(0)$, can then be measured as a function of sucrose concentration and a plot of $\sqrt{I(0)}$ *versus* electron density of the sucrose solution should give a straight line which can be extrapolated to find the electron density corresponding to zero scattered intensity.

This was done for the bottom component of WCMV. Scattered intensities in the forward direction were found by making intensity measurements at a number

of angles in the region of the Gaussian approximation and extrapolating to zero angle with a straight line extrapolation on a plot of log $I(\theta)$ *versus* θ. The results for $\sqrt{I(0)}$ as a function of the electron density of the sucrose solution are shown in Fig. 5. The electron density corresponding to zero intensity is 0.412 electron/Å^3. This is 1.23 times the electron density of water. The difference between this result and the value of 1.26 obtained above is within experimental error.

DISCUSSION

Recent work has shown that tomato bushy stunt virus (Caspar, 1956), turnip yellow mosaic virus (Klug, Finch, and Franklin, 1957), southern bean mosaic virus (Magdoff, 1960), poliovirus (Finch and Klug, 1959), and other so called "spherical viruses" are made up of a number of subunits arranged in some symmetrical way. Klug and Finch (1960) have shown that this symmetry is more pronounced in the top component than in the virus particle for the case of TYMV. These findings have led to virus models consisting of a number of small spheres arranged symmetrically on the faces or vertices of regular polyhedra. These structures closely resemble hollow spheres and it is assumed that they represent the protein shell inside which is packed the viral nucleic acid. The symmetry findings, however, do not require that the subunits be spherical. They might have an elongated shape which would cause them to extend further toward the center of virus, in which case the nucleic acid and the protein would overlap radially.

The density distributions presented here indicate that there is little or none of this overlapping in WCMV. The protein of the top component is very largely confined to a shell about 35 Å thick. There is indication of some increased density extending almost to the center of the molecule; however, it must be remembered that the top component preparation used for these studies was a mixture of two particles, one containing no nucleic acid and one containing 11 per cent RNA by weight. The material inside a radius of 105 Å could be the RNA of this latter particle. It will be interesting to obtain scattering data on a purified preparation of the particle with no nucleic acid.

Yamazaki and Kaesberg (1961*b*) found that the protein subunits of WCMV have a molecular weight of about 21,000. Assuming that these subunits occupy a volume given by the product of their molecular weight and the partial specific volume of top component, 0.74, then one calculates that if they were spherical they would have a diameter of 37 Å. The close agreement between this diameter and the value of 35 Å for the thickness of the protein shell in WCMV indicates that if the subunits are nearly spherical then their centers must all lie at very nearly the same distance from the center of the particle. If, however, the top component is made up of such subunits, then the scattering curve for top component should be modulated by the transform of a 37 Å sphere, which means that there should be a minimum in the scattering curve at 59 milliradians and a maximum at 76 milli-

radians. These features are not evident in the scattering curve for top component (Fig. 3). This would seem to indicate that the subunits are not spherical.

Finally a comment should be made about the agreement between the measured radii of gyration and those calculated for the models based on the Fourier transforms. The measured values are 112 Å and 135 Å for bottom and top component. The radius of gyration of a uniform sphere of 140 Å radius is 108 Å. The radius of gyration of a hollow sphere with an inner radius of 105 Å and an outer radius of 140 Å is 124 Å. Thus the measured values are 4 per cent and 8 per cent higher than the calculated values. There is some indication that aggregation of the virus might be a factor in this difference. Radius of gyration measurements on bottom component at the isoelectric point, pH 6.7, gave a much higher result of about 135 Å and an ultracentrifuge run at this pH showed the main peak due to bottom component and in addition another faster sedimenting peak which could have been an aggregation product.

This work was aided by grants from the National Institutes of Health.

Received for publication, June 19, 1961.

REFERENCES

BEEMAN, W. W., KAESBERG, P., ANDEREGG, J. W., and WEBB, M. B., 1957, *in* Handbuch der Physik, (S. Flugge, editor), Berlin, Springer-Verlag, **32**, 321.

CASPAR, D. L. D., 1956, *Nature*, **177**, 476.

FINCH, J. T., and KLUG, A., 1959, *Nature*, **183**, 1709.

GEIL, P. H., 1956, Ph.D. thesis, University of Wisconsin.

KLUG, A., and FINCH, J. T., 1960, *J. Molecular Biol.*, **2**, 201.

KLUG, A., FINCH, J. T., and FRANKLIN, R. E., 1957, *Biochim. et Biophysica Acta*, **25**, 242.

LEONARD, B. R., ANDEREGG, J. W., SHULMAN, S., KAESBERG, P., and BEEMAN, W. W., 1953, *Biochim. et Biophysica Acta*, **12**, 499.

MAGDOFF, B. S., 1960, *Nature*, **185**, 673.

MARKHAM, R., 1951, *Discussions Faraday Soc.*, **11**, 221.

MARKHAM, R., and SMITH, K. M., 1949, *Parasitology*, **39**, 330.

SCHMIDT, P., KAESBERG, P., and BEEMAN, W. W., 1954, *Biochim. et Biophysica Acta*, **14**, 1.

SINCLAIR, J. B., GEIL, P. H., and KAESBERG, P., 1957, *Phytopathology*, **47**, 372.

YAMAZAKI, H., and KAESBERG, P., 1961*a*, *Biochim. et Biophysica Acta*, **51**, 9.

YAMAZAKI, H., and KAESBERG, P., 1961*b*, *Biochim. et Biophysica Acta*, in press.